narraj

Original Article

Therapeutic potential of hUC-MSC secretome preconditioned with IFN-γ and/or TNF-α: An in vitro study on Alzheimer's neuronal cell models

Edhijanto Widaja[1,2*], Jeanne A. Pawitan[3,4,5] and Yetty Ramli[6]

[1]Department of Biomedical Science, Faculty of Medicine, Universitas Indonesia, Jakarta, Indonesia; [2]Regenerative Medicine and Research Institute, Mandaya Hospital Group, Tangerang, Indonesia; [3]Department of Histology, Faculty of Medicine, Universitas Indonesia, Jakarta, Indonesia; [4]Stem Cell Medical Technology Integrated Service Unit, Cipto Mangunkusumo Central Hospital, Jakarta, Indonesia; [5]Stem Cell and Tissue Engineering Research Cluster, Indonesia Medical Education and Research Institute (IMERI), Faculty of Medicine, Universitas Indonesia, Jakarta, Indonesia; [6]Department of Neurology, Faculty of Medicine, Universitas Indonesia, Jakarta, Indonesia

*Corresponding author: edhiyanto@gmail.com

Abstract

Alzheimer's disease is a progressive neurodegenerative disease that is characterized by toxic Amyloid-β (Aβ) plaques and neurofibrillary tangles (NFTs). Treatment options include the use of human umbilical cord mesenchymal stem cell (hUC-MSC)-based therapy. Its secretome contains healing substances such as neprilysin (CD10), which breaks down Aβ42; anti-inflammatory cytokines, which lower inflammation; and growth factors, which promote neuronal regeneration. The aim of this study was to produce hUC-MSC secretomes preconditioned with tumor necrosis factor-alpha (TNF-α) and/or interferon-gamma (IFN-γ) to enhance the secretion of these healing substances. hUC-MSCs were sub-cultured in T-25 flasks at a seeding density of 5×10^3 cells/cm² in 10 mL xeno-free medium. hUC-MSCs were preconditioned with TNF-α only, IFN-γ only, and a combination of TNF-α and IFN-γ. This study used 10 ng/mL TNF-α and 20 ng/mL IFN-γ. The secretome was harvested after 48 hours of preconditioning and then filtered through a 0.22 µm filter. In vitro tests were conducted to assess the effects of the secretome on neuronal survival using the neuroblastoma SH-SY5Y cell line. These cells were differentiated with retinoic acid (RA) and then exposed to Aβ42 to mimic Alzheimer's disease neurons. Secretome therapy was applied at concentrations of 5%, 10%, and 20% to evaluate neuroprotective effects. Four types of secretome were tested: unpreconditioned, TNF-α preconditioned, IFN-γ preconditioned, and a combination of TNF-α and IFN-γ. High levels of CD10 (neprilysin) expression were observed in hUC-MSCs treated with IFN-γ and TNF-α, although they did not release sufficient soluble neprilysin (sNEP). Viability results indicated that secretomes preconditioned with IFN-γ at 10% and 20% concentrations provided the highest increase in cell viability after 72 hours post-therapy. The combination of TNF-α and IFN-γ preconditioned secretome exhibited synergistic effects, particularly at 5% and 10% doses at 24- and 72-hours post-therapy. In conclusion, preconditioned hUC-MSC secretome represents a promising therapeutic approach for Alzheimer's disease, as it enhances neuronal cell viability and promotes neuronal regeneration. However, further studies are required to optimize sNEP release and maximize therapeutic efficacy in in vivo models.

Keywords: Alzheimer's, cell therapy, hUC-MSC, neprilysin, secretome

Introduction

Alzheimer's disease (AD) is the most common and widespread progressive neurodegenerative disease in the world, accounting for 60–70% of dementia cases [1]. AD-related dementia cases

https://narraj.org/

Received: February 14, 2025 - Accepted: April 25, 2025 - Published online: May 24, 2025

are rapidly increasing worldwide, with an estimated 55 million people diagnosed with dementia [2]. AD is the sixth leading cause of death in the world and the leading cause of dementia in the elderly [3]. AD is characterized by two pathological features: the accumulation of toxic amyloid-β42 (Aβ42) plaques on the outside of nerve cells, which then lead to the formation of neurofibrillary tangles (NFTs) within the nerve microtubules [4]. The accumulation of this abnormal protein leads to memory loss and cognitive dysfunction in patients, including progressive cognitive impairment, disorientation, and behavioral disorders [5,6]. In severe cases, these cognitive and behavioral changes could significantly impact a person's ability to function independently [7,8]. Brain damage in AD patients can lead to the failure to control the function of the body's organs, especially in the late stages of the disease, which may result in death [9].

Neuroinflammation and oxidative stress are critical contributors to AD pathogenesis. Microglial activation, a hallmark of neuroinflammation, exacerbates the deposition of amyloid-β (Aβ) plaques and tau protein pathology, further accelerating neurodegeneration [10,11]. Oxidative stress also contributes to the development of AD through macromolecular peroxidation or metal ion redox reactions or mitochondrial dysfunction, all of which affect cellular homeostasis, formation of reactive oxygen species (ROS), regulation of Aβ42 formation, and regulation of Tau protein formation [12-14]. Together, these processes create a vicious cycle of inflammation and oxidative damage that drives AD progression.

To mitigate these pathological effects, neprilysin (NEP) enzyme, also known as CD10, acts as a zinc metalloendopeptidase that plays a crucial role in degrading Aβ42 peptides [15,16]. NEP has a high affinity for Aβ42 and cleaves the peptide at the amine side of hydrophobic amino acids, leading to a rapid reduction in Aβ40 and Aβ42 levels [17]. As a type II integral membrane protein, NEP could undergo ectodomain shedding, releasing a soluble form (sNEP) into circulation [18]. This sNEP could potentially be utilized to degrade Aβ42 in the brains of AD patients.

Studies have shown that human umbilical cord mesenchymal stem cells (hUC-MSCs) could express NEP [16,19,20] and naturally secrete anti-inflammatory cytokines that help reduce neuroinflammation in AD patients [21,22]. Additionally, a study suggested that mesenchymal stem cells (MSCs) can be preconditioned to enhance the secretion of specific cytokines and proteins [23]. By optimizing this preconditioning, MSC-derived secretome may offer a promising therapeutic approach for AD through enhanced NEP activity and anti-inflammatory [24,25] effects.

The aim of this study was to evaluate the therapeutic potential of secretome derived from preconditioned hUC-MSC with tumor necrosis factor-alpha (TNF-α), interferon-gamma (IFN-γ), and their combination for AD. Specifically, the aims of this study were: (a) to assess the ability of these secretomes to degrade toxic Aβ42 peptides through sNEP activity and to determine their impact on reducing Aβ42 accumulation in an in vitro AD neuronal model; (b) to analyze the anti-inflammatory effects of secretome by measuring cytokine levels and their ability to suppress neuroinflammation; (c) to determine their neuroprotective properties by evaluating their effect in improving the levels of growth factors important for promoting neuronal survival and regeneration, such as glial cell line-derived neurotrophic factor (GDNF), brain-derived neurotrophic factor (BDNF), nerve growth factor (NGF), and vascular endothelial growth factor (VEGF); and (d) to assess the impact of secretome treatment on neuronal viability and apoptosis. This study also optimized the preconditioning conditions of hUC-MSC, identifying the best inducers to enhance NEP production and maximize the therapeutic effects of the secretome. These findings could contribute to the development of a novel cell-free therapy for AD.

Methods

Study design and setting

An in vitro study was conducted to test specific secretome produced from preconditioning hUC-MSCs with IFN-γ, TNF-α or their combination. It was hypothesized that the produced secretome would have a higher content of NEP, anti-inflammatory cytokines, and growth factors compared to standard unconditioned secretome. Therefore, this specific secretome was hypothesized to have better therapeutic effects against AD.

To test the therapeutic effect of this specific secretome, an AD neuronal cell model using neuroblastoma SH-SY5Y cells was employed. The SH-SY5Y cells were preconditioned with retinoic acid (RA) to differentiate into neuron-like cells. These cells were then exposed to Aβ42, which is a toxic and pathogenic protein for neuronal cells, such as in the brains of AD patients. Therefore, these neuron-like cells mimicked the condition of neuronal cells in AD patients. It was hypothesized that in the absence of secretome, these AD neuronal cell models would experience apoptosis or necrosis. By introducing the secretome containing sNEP into the culture, the Aβ42 peptides would be degraded, effectively reducing their accumulation and toxicity. This degradation might prevent the cells from being exposed to a toxic environment, thereby preserving cellular homeostasis and improving the viability of the neuron-like cells. As a result, the therapeutic effect of the secretome could be demonstrated through increased survival rates and enhanced health of the neuronal cells in comparison to untreated controls.

Three variations of specific secretome were prepared: those derived from hUC-MSC preconditioned with IFN-γ, preconditioned with TNF-α, and preconditioned with a combination of IFN-γ and TNF-α. Three different doses of secretome were used: 5%, 10%, and 20% of the medium volume. The design of the study is presented in **Figure 1**.

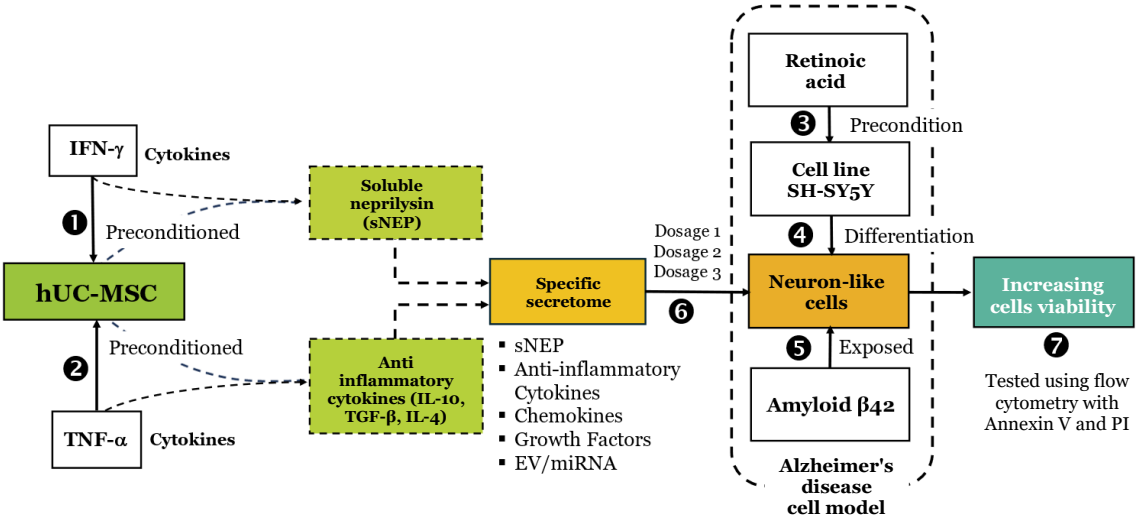

Figure 1. Study design and setting of the study.

Sub-culture of hUC-MSC cells

Before use, human umbilical cord-derived mesenchymal stem cells (hUC-MSCs) were evaluated for compliance with the International Society for Cell & Gene Therapy (ISCT) criteria for mesenchymal stem cells, which included adherence to plastic, trilineage differentiation potential, and expression of specific surface markers (≥95% positive for CD73, CD90, and CD105, and ≤2% negative for CD34, CD45, CD14 or CD11b, CD79α or CD19, and HLA-DR). Flow cytometric characterization of hUC-MSCs was performed using the BD FACSAria III (BD Biosciences, USA).

The hUC-MSCs were sub-cultured in a T-25 flasks (25 cm^2) with 10 mL of xeno-free culture medium. A seeding density of 5×10^3 cells/cm^2 was used, and the culture medium was prepared following the protocol by Pawitan *et al.* [26]. The α-Minimum Essential Medium (α-MEM) (Gibco, Grand Island, USA) was used together with 10% volume of Human Platelet Lysate (HPL), fibrinogen-depleted, xeno-free (StemCell Technologies, Vancouver, Canada), 1% volume of GlutaMax Supplement (Gibco, Grand Island, USA), and 1% volume of antibiotic-antimycotic solution (Sigma-Aldrich, St. Louis, USA).

Preconditioning hUC-MSC to produce specific secretome

Four types of secretome were generated: unpreconditioned, preconditioned with TNF-α alone, preconditioned with IFN-γ alone, and preconditioned with a combination of TNF-α and IFN-γ. The hUC-MSCs were preconditioned with 20 ng/mL IFN-γ to enhance NEP expression and stimulate the production of anti-inflammatory cytokines. Human recombinant IFN-γ (animal-component free, ACF) from Stemcell Technologies was used (Catalog No. 78141.1, Vancouver,

Canada). For TNF-α preconditioning, hUC-MSCs were treated with 10 ng/mL Human Recombinant TNF-α (ACF) (Catalog No. 78157.1, Stemcell Technologies, Vancouver, Canada). For the combination, 20 ng/mL IFN-γ and 10 ng/mL TNF-α were used. All preconditioned hUC-MSCs were incubated for 48 hours at 37°C and 5% CO_2.

Measuring the impact of preconditioning on neprilysin expression

It was predicted that UC-MSC preconditioning with TNF-α and/or IFN-γ would modulate the NEP production. To quantify NEP expression, flow cytometry was performed by measuring the mean fluorescence intensity (MFI) of a fluorescein isothiocyanate (FITC)-tagged monoclonal antibody against NEP. The FITC emits green light when excited by blue light, with an excitation maximum of 495 nm and an emission maximum of 519 nm [27]. MFI was used to determine the expression level of NEP on the cell surface. By comparing the MFI of a stained sample to that of a control, relative changes in expression were measured [28]. Relative MFI was calculated by subtracting the MFI of the control—representing cells without NEP monoclonal antibody staining—from that of the stained sample. This approach was used to provide a quantitative measure of NEP expression on the cell surface. Given that NEP undergoes cleavage to generate sNEP, which retains enzymatic activity, the secretome containing sNEP was further evaluated for its ability to degrade toxic Aβ42 peptides. Since Aβ42 accumulation is highly toxic to neuronal cells and leads to cell death, the impact of reducing Aβ42 was assessed by measuring cell viability. Higher cell viability in treated samples would indicate a reduction in Aβ42-induced toxicity, supporting the potential neuroprotective role of the secretome. For NEP measurement, the reagent CD10 Monoclonal Antibody LT10 FITC (Invitrogen, Carlsbad, USA) was used.

Secretome harvesting

After 48 hours, the flask was removed from the incubator, and secretome isolation was performed following the protocol described by Gorgun *et al.* [29], with modifications, as illustrated in **Figure 2**. The conditioned medium, referred to as the secretome, was filtered using a 0.22 µm filter to ensure complete removal of cells. A Millex-OR Filter Unit (Merck, Darmstadt, Germany) was used for filtration. The filtered secretome was then stored at -80°C in a deep freezer to preserve the stability and biological activity of its bioactive components [30,31], including proteins, enzymes, cytokines, and growth factors.

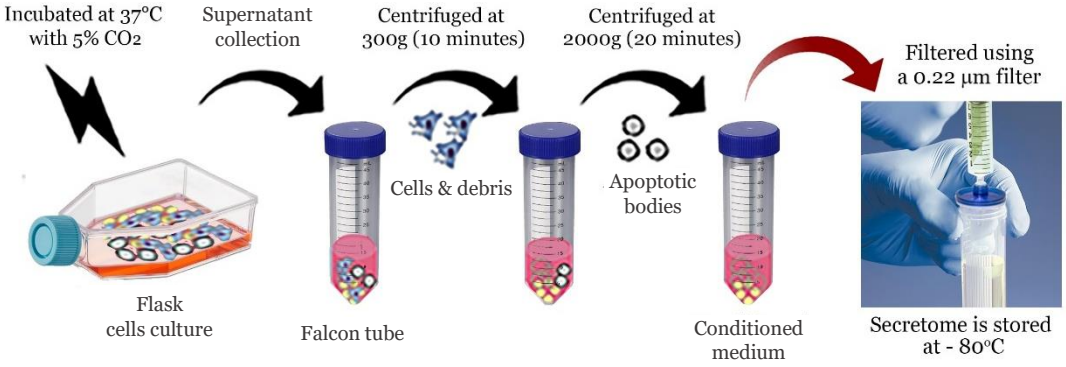

Figure 2. Main steps of secretome isolation process.

Secretome characterization

To investigate the potential anti-inflammatory and neuroprotective properties of the secretome, its bioactive components were analyzed including sNEP, anti-inflammatory cytokines (IL-4, IL-10, and TGF-β), and neurotrophic growth factors (BDNF, GDNF, NGF, and VEGF). Quantification was performed using enzyme-linked immunosorbent assay (ELISA) for sNEP, VEGF, and TGF-β, and a multiplex assay based on Luminex xMAP technology for BDNF, GDNF, NGF, IL-4, and IL-10.

sNEP concentrations were measured using the Human Neprilysin (MME) ELISA Kit (Invitrogen, Carlsbad, USA). BDNF, GDNF, NGF, IL-4, and IL-10 levels were quantified using the Human Magnetic Luminex Assay, Premixed Multiplex (Bio-Techne, Minneapolis, MI, USA). TGF-β1 level was assessed using the Human TGF-β1 Quantikine ELISA Kit (Bio-Techne,

Minneapolis, MI, USA), and VEGF levels were measured using the Human VEGF Quantikine ELISA Kit (Bio-Techne, Minneapolis, MI, USA). All assays were conducted in accordance with the manufacturer's protocols.

Alzheimer's disease neuronal cell modeling

To establish an AD neuronal cell model, the SH-SY5Y neuroblastoma cell line was obtained from the European Collection of Authenticated Cell Cultures (ECACC) (SA 94030304-1VL, Sigma-Aldrich, Merck, Darmstadt, Germany). The cryopreserved SH-SY5Y cells were thawed and seeded at a density of 7,500 cells/cm^2 for expansion.

SH-SY5Y neuroblastoma cells were preconditioned with RA (SA R2625-50MG, Sigma-Aldrich, Darmstadt, Germany) to induce differentiation into neuron-like cells. Briefly, SH-SY5Y cells were seeded in 24-well plates at a density of 1.0×10^4 to 1.0×10^5 cells/cm^2. RA was administered at a concentration of 10 µM (3 mg/mL) for four days (96 hours). Preconditioning with RA was terminated after the fourth day upon observing a substantial number of neuron-like cells. These neuron-like cells were then exposed to 0.82 mg/mL of Aβ42 peptide. The Aβ42 peptide used was the human beta-amyloid 1-42 protein transduction domain recombinant (03-112, Thermo Fisher, Waltham, MA, USA). Exposure to Aβ42 was not discontinued; rather, its effects were observed on neuron-like cells that were either untreated or treated with various types of preconditioned secretome.

Since it was expected that the neuron-like cells exposed to Aβ42 underwent apoptosis, post-exposure cell viability was then assessed using flow cytometry with the Annexin V-FITC/PI Apoptosis Kit (Elabscience, Wuhan, China).

Evaluating the effects of secretome on cell viability of Alzheimer's disease neuronal cell model

Four types of secretome at three concentrations (5%, 10%, and 20%) were introduced into cultures of AD neuronal cell model (neuron-like cells exposed to Aβ42) for 24, 48, and 72 hours. This resulted in 14 treatment groups: secretome without preconditioning (three doses), secretome preconditioned with TNF-α (three doses), secretome preconditioned with IFN-γ (three doses), secretome preconditioned with a combination of TNF-α and IFN-γ (three doses), a positive control (normal neuronal cells), and a negative control (AD neuronal cell model). Sample size was determined using Walter T. Federer's formula [32], yielding three replicates per group.

The cell viability was then assessed using flow cytometry with the Annexin V-FITC/PI Apoptosis Kit (Elabscience, Wuhan, China). Analysis focused on viable cells (Quadrant 3), assuming that cells outside this quadrant were either undergoing apoptosis or necrosis. The viability of the cells was evaluated at 24, 48, and 72 hours post-secretome treatment.

Morphological assessment of neuronal cell model pre and post therapy

To confirm the differentiation of SH-SY5Y neuroblastoma cells into neuron-like cells following RA preconditioning, morphological observations were performed on the third day. A Nikon Eclipse Ti inverted microscope (Nikon Corporation, Tokyo, Japan) was used at different magnifications: 40× to assess cell density, 200× to examine cellular interactions, and 400× to observe detailed structures such as neurons, axons, and dendrites. This served as a pre-therapy morphological assessment of the neuronal cell model.

The morphology, density, and overall health of the AD neuronal cell model were then re-assessed at 48 and 72 hours post-secretome treatment. This evaluation aimed to determine apoptosis persistence and to assess whether an improved microenvironment enhanced neuronal viability and function. These observations provided insights into the therapeutic potential of secretome in promoting neuronal survival and regeneration, potentially mitigating neurodegeneration.

Statistical analysis

One-way ANOVA was performed to determine whether sNEP, cytokine, and growth factor levels differed significantly among the various secretome types. Post hoc tests were conducted to identify specific group differences following ANOVA. Multiple comparison procedures were applied to evaluate differences in group means or medians. Tukey's Honest Significant Difference

(HSD) test was used when the assumption of homogeneity of variance was met. For data that were not normally distributed, non-parametric tests, such as the Kruskal–Wallis test, were utilized as appropriate. Pearson correlation analysis was used to assess potential correlations between cytokines and growth factors. All statistical analyses were conducted using IBM SPSS Statistics, Version 26 (IBM Corp., Armonk, NY, USA).

Results

Phenotypic confirmation of hUC-MSCs

hUC-MSC cultures exhibited fibroblast-like morphology, a characteristic of mesenchymal stem cells [33,34]. Flow cytometry analysis revealed that CD90+ expression was 100%, CD73+ was 99.9%, and CD105+ was 99.6%, while Lineage (-) expression was 1.3%. The results indicate that the hUC-MSCs used as the source of the secretome met the standards set by the International Society for Cellular Therapy (ISCT) for mesenchymal stem cells [34].

Neprilysin (CD10) levels in the four types of secretome

MFI values for the four secretome types, indicating NEP protein expression levels on the cell surface, are presented in **Figure 3**. One-way ANOVA revealed a statistically significant difference in relative MFI among the groups ($p<0.05$). NEP expression was highest in hUC-MSCs preconditioned with IFN-γ and lowest in those induced with TNF-α. The IFN-γ–preconditioned group exhibited the greatest MFI, suggesting the highest level of membrane-bound NEP. This upregulation was significantly greater compared to the other preconditioning groups and the unconditioned control.

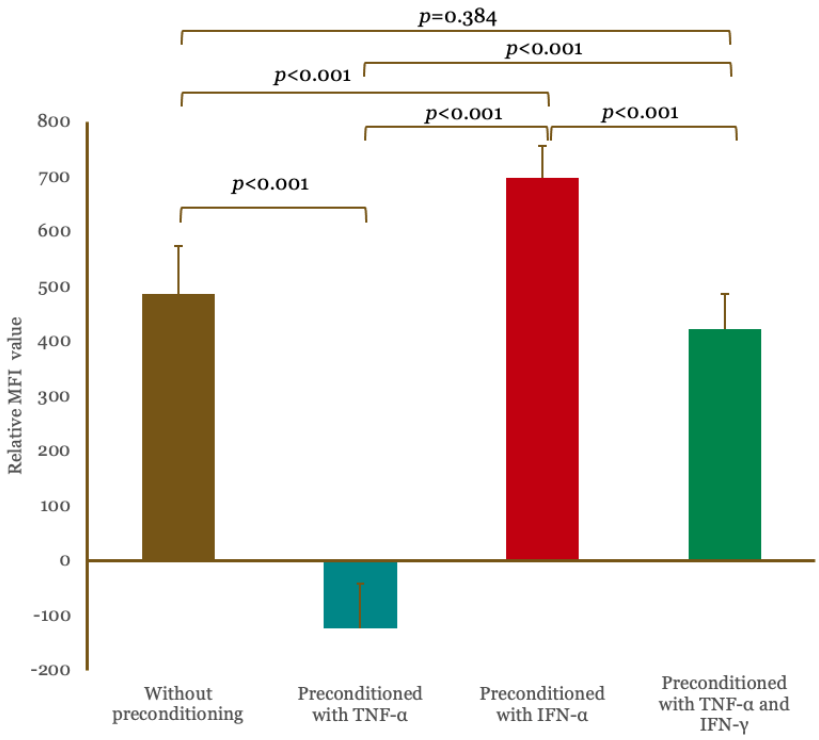

Figure 3. Comparison of relative mean fluorescence intensity (MFI) indicating neprilysin (CD10) expression among different types of secretome.

Comparison of sNEP levels among the four types of secretome

The results for sNEP levels are presented in **Figure 4**. Statistical analysis using the Kruskal–Wallis test yielded a p-value of 0.554, indicating no statistically significant differences among the four secretome types. In contrast, analysis of membrane-bound CD10/NEP expression revealed significant differences in response to the various secretome treatments.

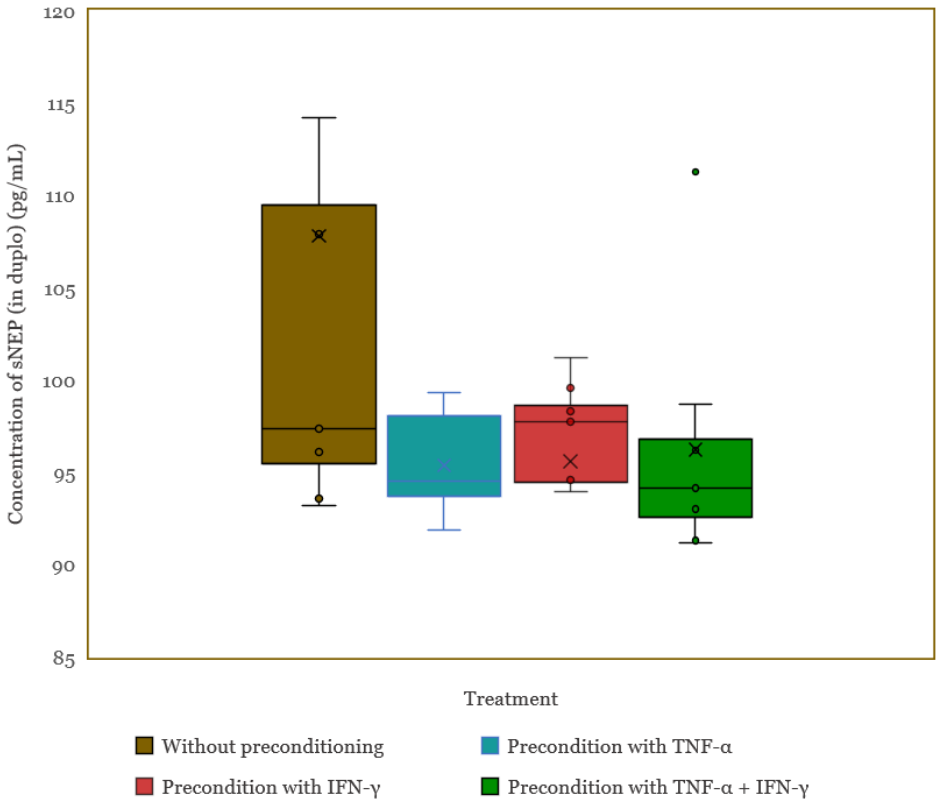

Figure 4. Comparison of soluble neprilysin (sNEP) levels among four types of secretome.

Comparison of IL-4 and IL-10 levels among the four types of secretome

The comparison of IL-4 concentrations across the four secretome types is presented in **Figure 5A**, while the comparison of IL-10 concentrations is presented in **Figure 5B**. Statistical analysis revealed no significant difference in IL-4 levels among the groups (p=0.772). Similarly, IL-10 levels did not exhibit any statistically significant variation between the secretome types (p=0.739).

Comparison of TGF-β levels among the four types of secretome

The comparisons of TGF-β levels across the different secretome types are presented in **Figure 6**. The Kruskal–Wallis test showed a significant difference in the levels of TGF-β only between the unconditioned secretome and the TNF-α–preconditioned group. These findings suggest that TNF-α preconditioning significantly enhances the secretion of the anti-inflammatory cytokine TGF-β.

The results indicated that differences in IL-4 and IL-10 levels were not statistically significant between secretome types. The reasons for the observed differences in TGF-β levels remain unclear. Pearson correlation analysis revealed that all correlations between variables were very weak and not statistically significant (p>0.05). These findings suggest that no meaningful associations were observed between the secretome type and the concentrations of IL-4, IL-10, or TGF-β in this study.

Comparison of BDNF, GDNF, and NGF among the four types of secretome

The comparison of BDNF concentrations across the different secretome types is presented in **Figure 7A**. Statistical analysis showed no significant difference in BDNF levels among the groups (p=0.083). In contrast, a statistically significant difference was observed among secretome types (p=0.006) in GDNF concentrations, as illustrated in **Figure 7B**. Post-hoc analysis using the Tukey HSD test revealed that this difference was specifically between the unconditioned secretome and the group preconditioned with a combination of TNF-α and IFN-γ. No significant differences were detected across the secretome types (p=0.424) in NGF levels, as presented in **Figure 7C**.

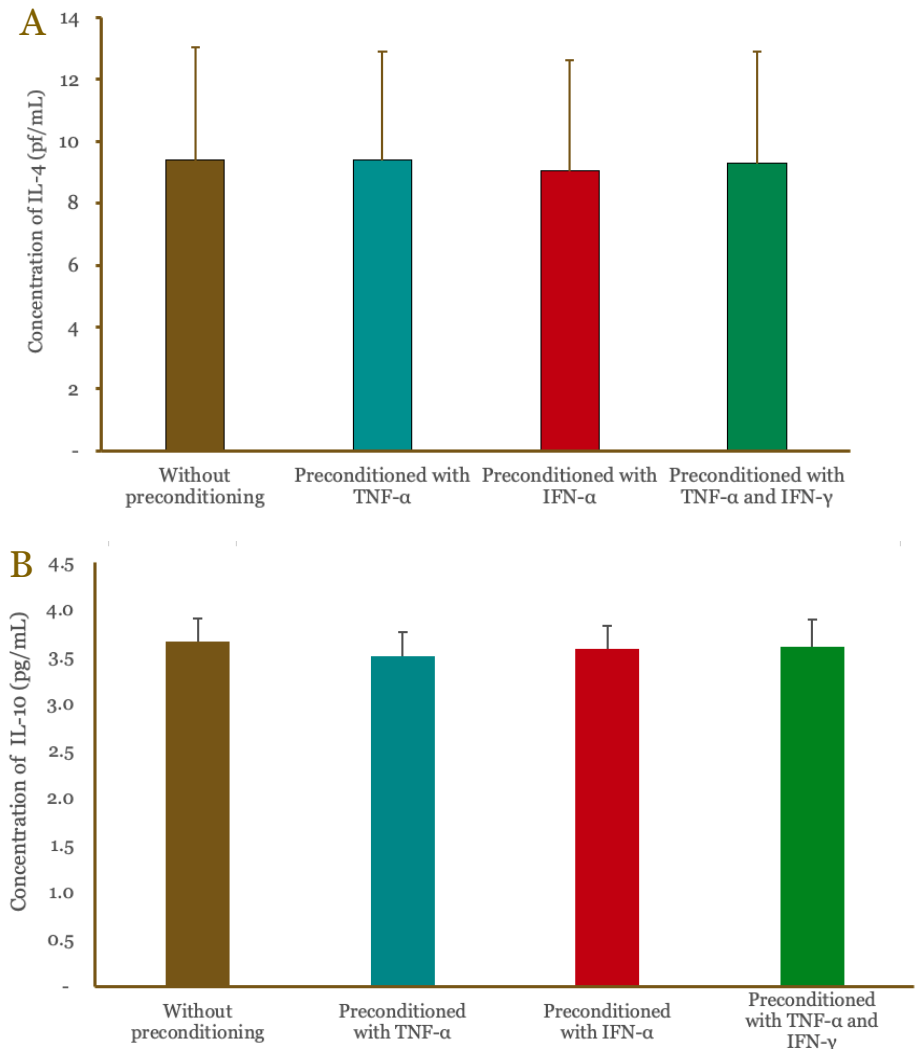

Figure 5. Comparison of IL-4 (A) and IL-10 (B) concentrations for each type of secretome.

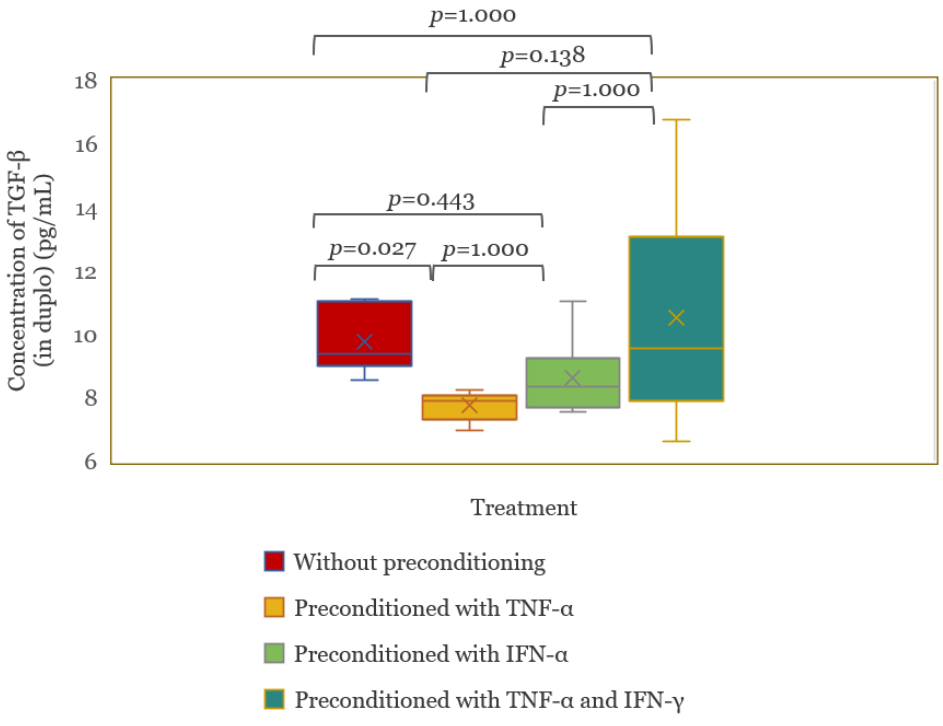

Figure 6. Comparison of TGF-β levels for each type of secretome.

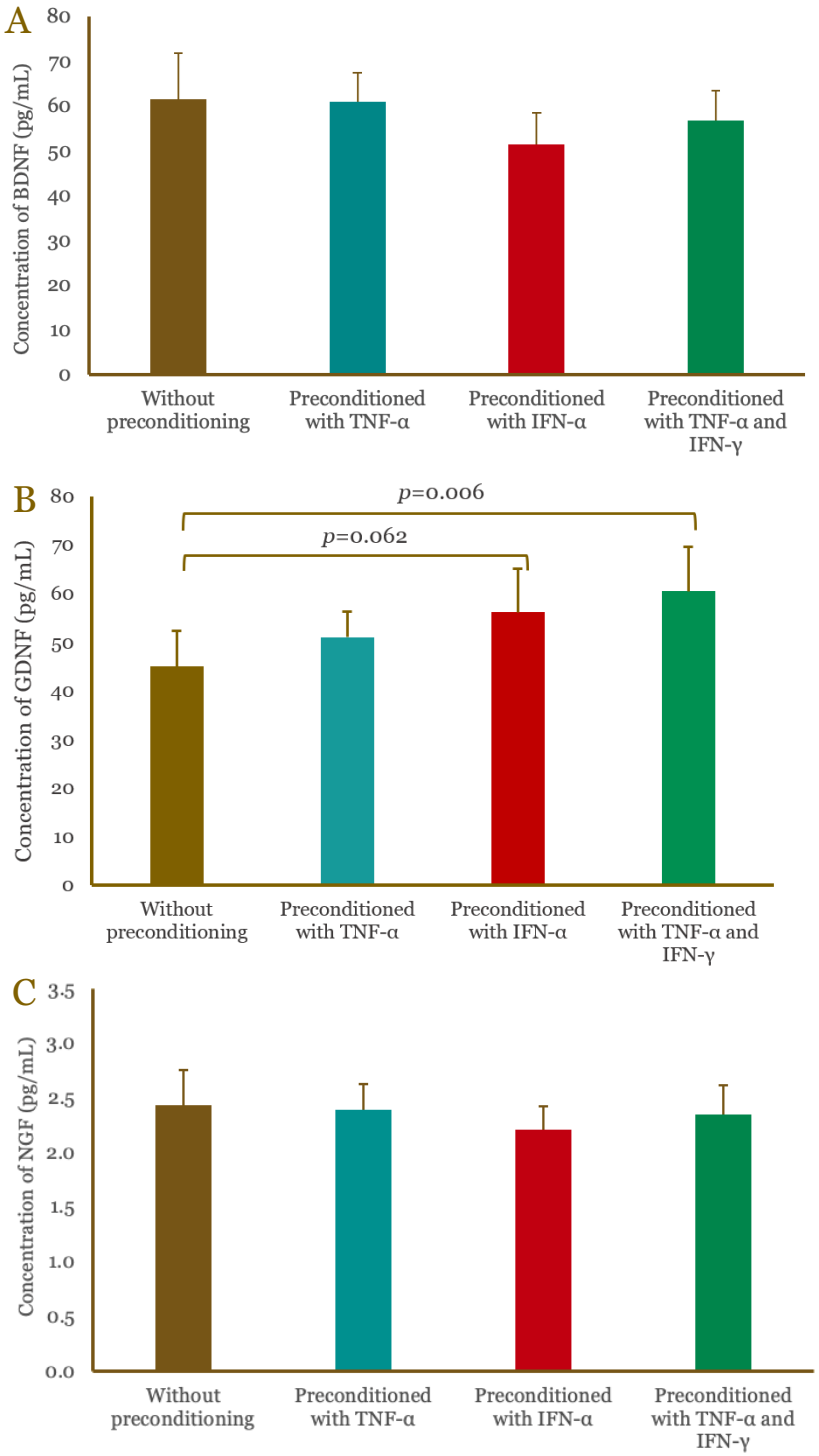

Figure 7. Comparison of (A) brain-derived neurotrophic factor (BDNF), (B) glial cell line-derived neurotrophic factor (GDNF), and (C) nerve growth factor (NGF) concentrations for each type of secretome.

Comparison of VEGF among the four types of secretome

The comparison of VEGF levels across different secretome types is presented in **Figure 8**. The independent-samples Kruskal-Wallis statistical test showed no significant difference in VEGF levels among the secretome types.

From the results of the growth factor analysis, no significant differences were observed among the secretome types, except for GDNF, which showed a statistically significant difference. The highest GDNF levels were obtained from hUC-MSCs preconditioned with a combination of TNF-α and IFN-γ. Among the growth factors, NGF secretion was the lowest, followed by VEGF, BDNF, and GDNF.

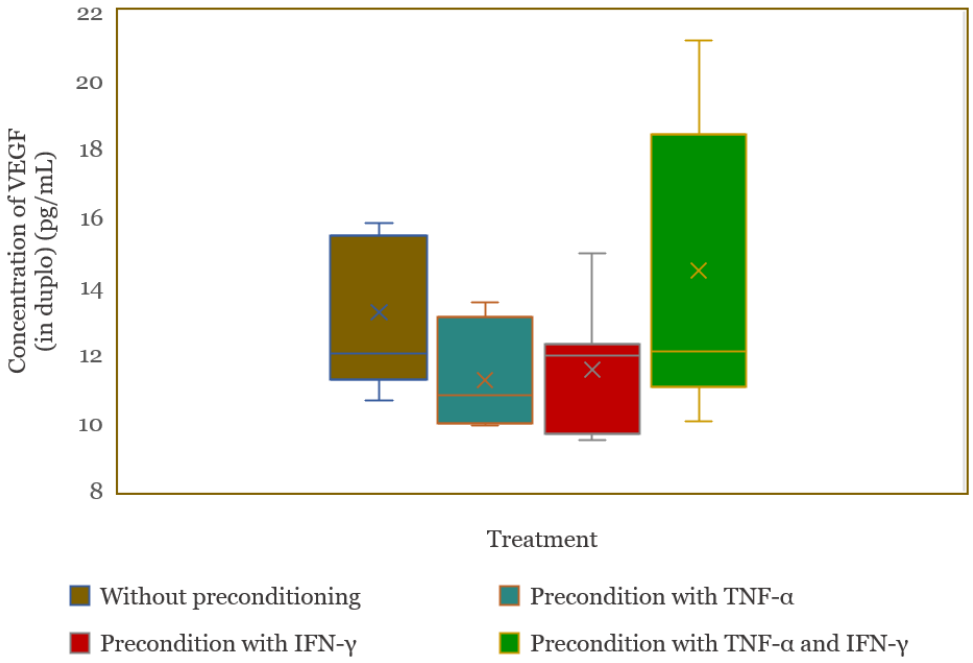

Figure 8. Comparison of vascular endothelial growth factor (VEGF) levels for each type of secretome.

Viability assay in an Alzheimer's neuronal cell model post secretome therapy

Cell viability in an Alzheimer's neuronal cell model following secretome treatment was assessed at 24 hours (**Figure 9A**), 48 hours (**Figure 9B**), and 72 hours (**Figure 9C**) post-treatment. At 24 hours, the secretome preconditioned with a combination of TNF-α and IFN-γ resulted in a higher viability rate compared to the untreated Alzheimer's condition, in which cell viability had declined to 38.17% due to Aβ42 exposure (**Figure 9A**). This finding indicates that TNF-α and IFN-γ preconditioning enhances the neuroprotective effect of the secretome, improving cell viability in the early post-treatment phase.

ANOVA analysis assessing the effect of secretome dose on cell viability showed no statistically significant difference (p=0.399). However, ANOVA results for secretome type revealed a statistically significant difference (p=0.023), indicating that the type of preconditioning influences therapeutic efficacy. Post hoc analysis identified a significant difference in cell viability between the secretome preconditioned with IFN-γ alone and the one preconditioned with the combination of TNF-α and IFN-γ.

At 48 hours post-treatment, all secretome types resulted in higher cell viability compared to the Alzheimer's condition, in which viability was reduced to 41.30% (**Figure 9B**). This suggests a general improvement in cell survival following secretome administration. The highest viability was observed with the 10% dose of secretome preconditioned with IFN-γ (**Figure 9B**). However, ANOVA analysis revealed no statistically significant effect of secretome dose on cell viability (p=0.144). Likewise, no significant difference in cell viability was observed among the different secretome types (p=0.713), indicating that neither dose nor secretome type produced a statistically distinct effect at this time point.

At 72 hours post-treatment, all secretome types at 10% and 20% doses resulted in higher cell viability compared to the Alzheimer's condition, in which viability was reduced to 55.60% (**Figure 9C**). The highest viability was observed in the group treated with the 10% dose of IFN-γ–preconditioned secretome, reaching 79.40%. This value was remarkably close to the viability of healthy control cells (81.23%), with a minimal difference of only 1.83% (**Figure 9C**). Despite these improvements, ANOVA analysis for secretome dose revealed no statistically significant differences in cell viability across the different doses (p=0.064). Similarly, the ANOVA test for secretome type indicated no significant differences among the treatment groups (p=0.415), suggesting that neither dose nor secretome type significantly affected cell viability at this time point.

Widaja et al. Narra J 2025; 5 (2): e2281 - http://doi.org/10.52225/narra.v5i2.2281

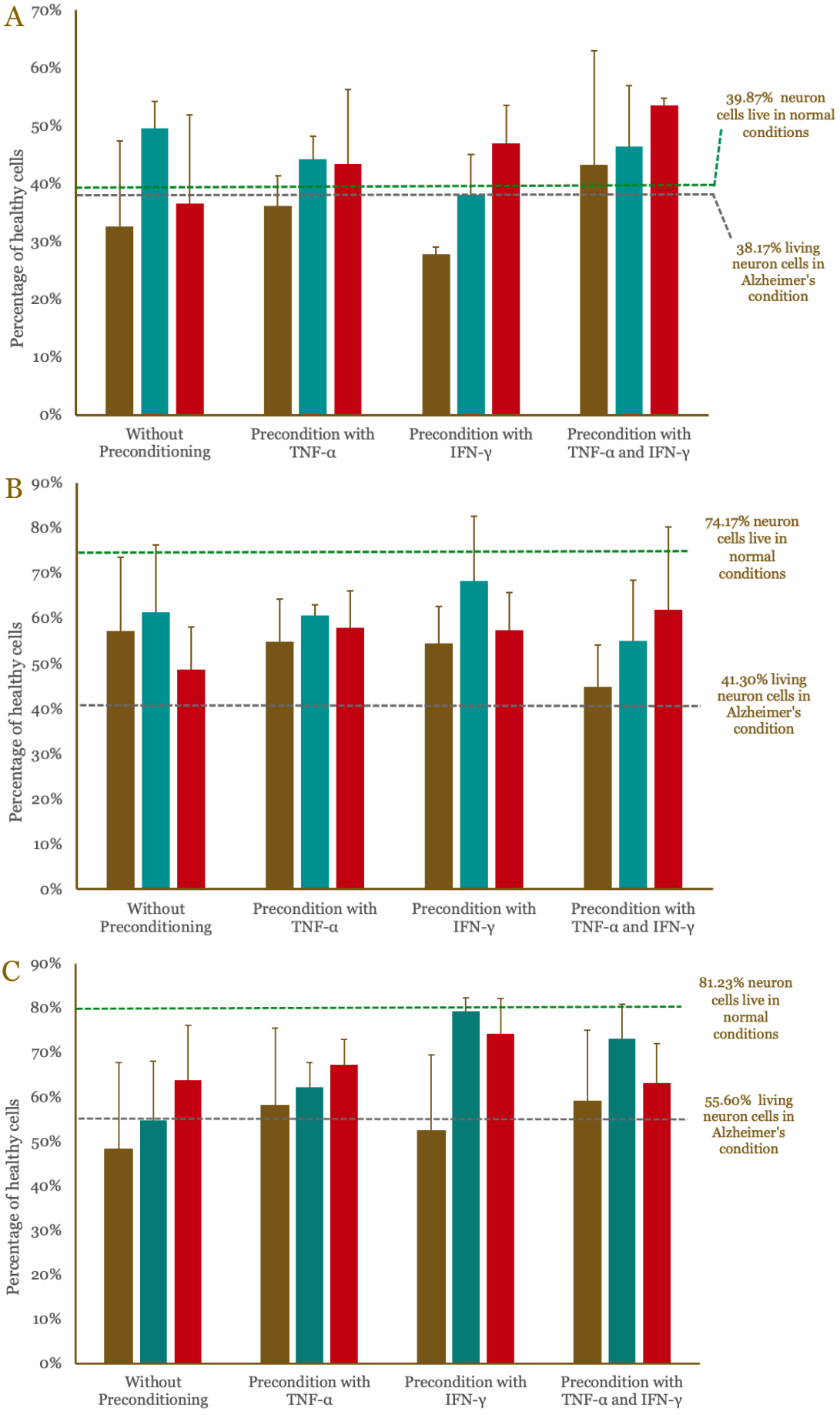

Figure 9. Percentage of viable cells in populations treated with four types of secretome at three different doses after 24 hours (A), 48 hours (B) and 72 hours (C).

Effect of secretome dose on cell viability over time

The increase in healthy cell numbers following treatment was evaluated at 24, 48, and 72 hours for the 5% secretome (**Figure 10A**), 10% secretome (**Figure 10B**), and 20% secretome (**Figure 10C**). For the 5% secretome, the non-preconditioned group exhibited the greatest increase in cell viability between 24 and 48 hours; however, a decline was observed at 72 hours (**Figure 10A**). In contrast, secretomes preconditioned with TNF-α or with a combination of TNF-α and IFN-γ exhibited a more consistent increase in cell viability over time, with the combination preconditioning yielding the highest viability at 72 hours (59.10%). Preconditioning with IFN-γ alone resulted in a substantial increase in viability between 24 and 48 hours, followed by stabilization at 72 hours. Among all groups, the secretome derived from hUC-MSCs preconditioned with TNF-α and IFN-γ produced the highest percentage of viable cells at 72 hours, followed by preconditioned with TNF-α alone. Although the non-preconditioned secretome maintained relatively high viability for up to 48 hours, its effect diminished by 72 hours (**Figure 10A**).

The viability test results for the 10% secretome dose, presented in **Figure 10B**, revealed that preconditioning with IFN-γ resulted in the highest percentage of viable cells (79.40%) at 72 hours post-treatment, indicating the most effective condition among all groups. Preconditioning with a combination of TNF-α and IFN-γ also led to a substantial increase in viability, reaching 73.27% simultaneously. In contrast, the non-preconditioned secretome demonstrated a steady increase in cell viability up to 48 hours, followed by a decline at 72 hours. Secretome preconditioned with TNF-α alone exhibited a consistent increase over time; however, its final viability at 72 hours remained lower compared to that observed with IFN-γ alone or the TNF-α and IFN-γ combination (**Figure 10B**). These findings suggest that IFN-γ preconditioning is the most effective approach for enhancing cell viability at a 10% secretome dose, particularly over longer durations. The combination of TNF-α and IFN-γ also produced promising outcomes, supporting its potential for further investigation in future studies.

For the 20% secretome dose, as illustrated in **Figure 10C**, preconditioning with IFN-γ resulted in the highest cell viability at 72 hours (74.33%), indicating it as the most effective strategy for enhancing the proportion of healthy cells at this dose. Preconditioning with TNF-α also produced consistent and favorable results, with viability reaching 67.27% at 72 hours post-treatment. The non-preconditioned secretome showed a steady increase in cell viability, although the improvement was less pronounced compared to the TNF-α– and IFN-γ–treated groups. Preconditioning with the combination of TNF-α and IFN-γ led to a notable increase in viability at 48 hours; however, the final viability at 72 hours was slightly lower than that achieved with IFN-γ alone (**Figure 10C**). These findings suggest that IFN-γ preconditioning at a 20% secretome dose is the most effective approach for sustaining cell viability over time, followed by TNF-α preconditioning.

Microscopic observation results of neuron-like cell formation

Cells that did not adhere to the bottom of the dish, suggesting that they may have perished prior to the initiation of the differentiation process, are presented in **Figure 11A** and **Figure 11B**. Most of the cells remain fibroblastic, resembling SH-SY5Y neuroblastoma cells, while a minor fraction has commenced differentiation into neuron-like cells following induction with RA.

Microscope observation 48 hours post-therapy

An intriguing phenomenon occurred 48 hours post-therapy, suggesting that the activity of the neprilysin enzyme had concluded and the cellular microenvironment had begun to ameliorate. Consequently, two concurrent processes emerged: proliferation, particularly of SH-SY5Y neuroblastoma cells, and differentiation, resulting in an increased formation of neuron-like cells (**Figure 12A**, **12B**, **12C**).

Microscope observation 72 hours post-therapy

An interesting phenomenon occurred 72 hours post-therapy, suggesting an enhancement in the microenvironment supporting the cells. Consequently, two concurrent processes were observed: proliferation, particularly in SH-SY5Y neuroblastoma cells, and increased differentiation of neuron-like cells (**Figure 13A**, **13B**, **13C**).

A

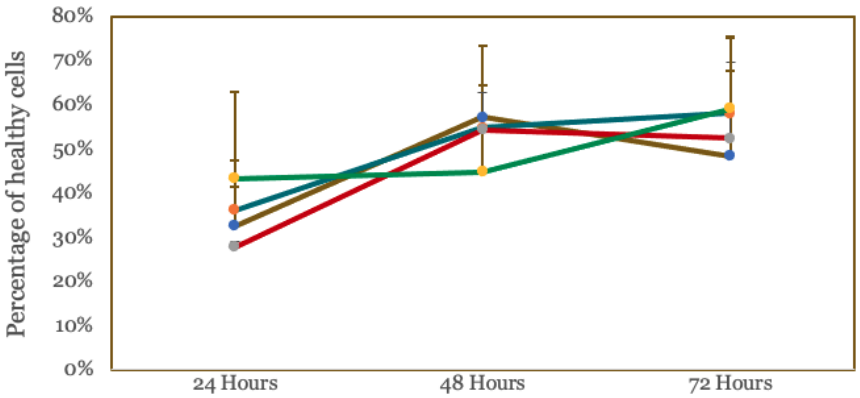

	24 Hours	48 Hours	72 Hours
Mean, without preconditioning	32.60%	57.20%	48.33%
Mean, precondition (TNF-α)	36.13%	54.80%	58.10%
Mean, precondition (IFN-γ)	27.80%	54.40%	52.37%
Mean, precondition (TNF-α, TFN-γ)	43.37%	44.87%	59.10%

Post-therapy observation time

B

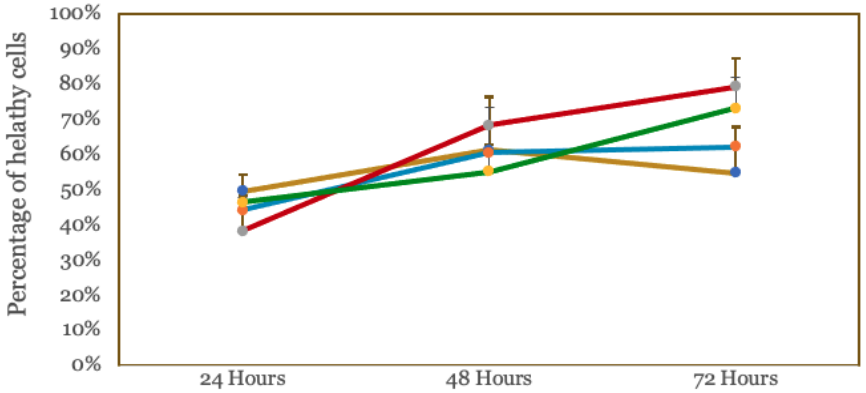

	24 Hours	48 Hours	72 Hours
Mean, without preconditioning	49.57%	61.27%	54.83%
Mean, precondition (TNF-α)	44.23%	60.60%	62.20%
Mean, precondition (IFN-γ)	38.17%	68.33%	79.40%
Mean, precondition (TNF-α, TFN-γ)	46.47%	55.07%	73.27%

Post-therapy observation time

C

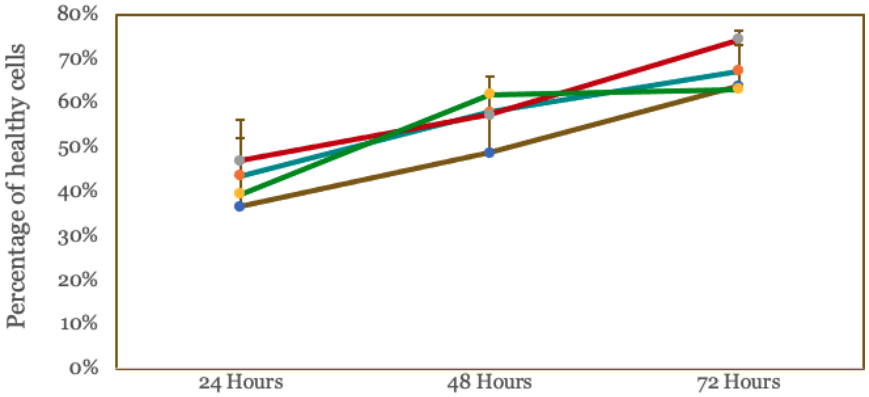

	24 Hours	48 Hours	72 Hours
Mean, without preconditioning	36.63%	48.67%	63.83%
Mean, precondition (TNF-α)	43.50%	57.87%	67.27%
Mean, precondition (IFN-γ)	46.97%	57.37%	74.33%
Mean, precondition (TNF-α, TFN-γ)	39.43%	61.90%	63.13%

Post-therapy observation time

Figure 10. Viability of cells treated with 5% (A), 10% (B), and 20% secretome (C), assessed at 24, 48, and 72 hours after treatment.

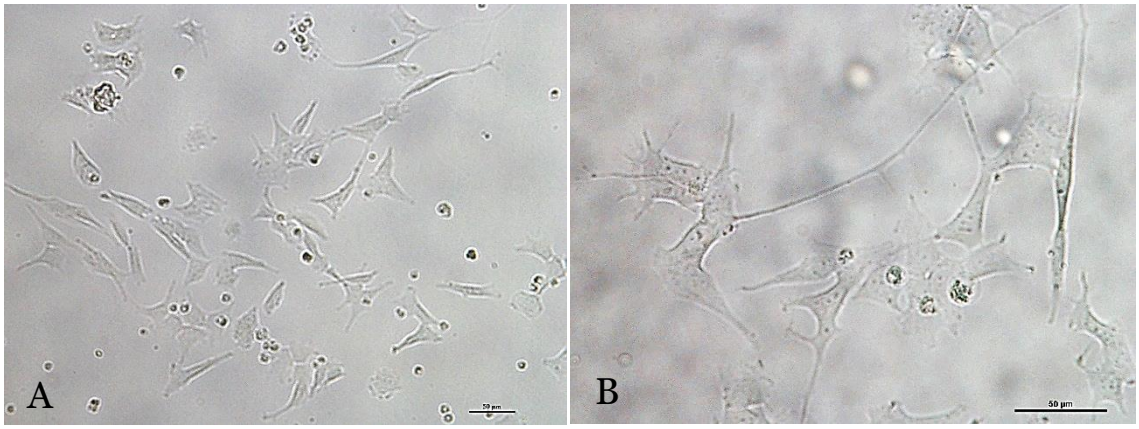

Figure 11. Representative microscopic images of SH-SY5Y cells on day three of retinoic acid (RA)-induced differentiation. Some cells retain a fibroblast-like morphology, while others exhibit neuronal characteristics, including soma and axon formation. (A) 200× magnification, (B) 400× magnification.

Figure 12. Representative microscopic images at 48 hours post-treatment showed increased cell proliferation and a higher number of morphologically differentiated cells. (A) 40× magnification, (B) 200× magnification, (C) 400× magnification.

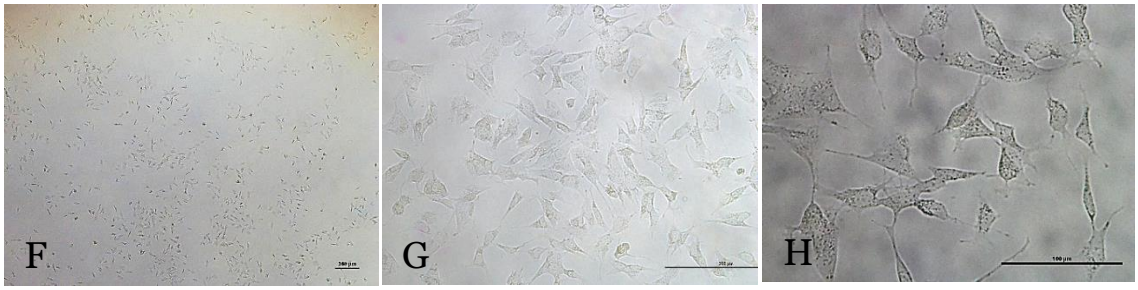

Figure 13. Representative microscopic images at 72 hours post-treatment, demonstrating enhanced cell proliferation and an increased number of morphologically differentiated cells. (A) 40× magnification, (B) 200× magnification, (C) 400× magnification.

Discussion

The highest relative MFI, reflecting the quantity of CD10 protein on the cell surface, was attributed to the secretome type group of hUC-MSC preconditioned by IFN-γ. This is in line with several studies conducted by other researchers who stated that IFN-γ can cause an increase in CD10 expression [19,35]. TNF-α induced metalloproteinase activity, leading to the cleavage and release of CD10 from the cell surface. Additionally, TNF-α triggered CD10 internalization via receptor-mediated endocytosis and downregulated its transcription through NF-κB signaling. This study demonstrated that IFN-γ enhanced CD10 (neprilysin) expression on hUC-MSCs, while TNF-α reduced surface CD10 levels, likely due to cleavage, release, or internalization via endocytosis. However, further analysis was required to confirm these mechanisms.

The neprilysin assay results showed no substantial variation in sNEP levels across the examined secretome types. The lack of increased sNEP levels, despite elevated CD10 expression

in hUC-MSCs preconditioned with various stimuli, could be explained by multiple interrelated biological pathways. This study demonstrated that although CD10 expression increased—indicating its association with neprilysin in the cell membrane—preconditioning with TNF-α did not lead to the expected release of neprilysin/CD10 into the culture medium as sNEP.

Literature reviews indicated that this release of CD10 from the cell surface was primarily facilitated by proteolytic enzymes known as matrix metalloproteinases (MMPs) [36]. The administration of TNF-α as a preconditioning factor in cell cultures was reported to enhance the activity of specific MMPs, such as MMP-3 and MMP-7, which play a critical role in the proteolytic cleavage of CD10. However, if these MMPs were not sufficiently activated by TNF-α or if their activity was inhibited, the release of sNEPs remained limited, despite high CD10 expression on the cell surface [37,38].

Additionally, previous studies suggested that hypoxic conditions could upregulated the expression of certain MMPs, particularly MMP-2 and MMP-9, through the HIF-1α pathway. Incubating cell cultures under hypoxia has been reported to naturally enhance MMP production, thereby facilitating the release of CD10 into sNEP in the culture medium [39]. However, this study did not investigate the effects of hypoxia due to the unavailability of a hypoxic incubator in the laboratory.

The findings of this study support the therapeutic potential of anti-inflammatory cytokines in mitigating neuroinflammation in AD. Prior studies by Kapoor, *et al*. [40] and Von Bernhardi, *et al*. [41] highlighted the role of IL-4, IL-10, and TGF-β in AD therapy, with TGF-β emerging as the most critical cytokine for inflammation control. This study demonstrated that TNF-α preconditioning induced greater anti-inflammatory cytokine secretion than IFN-γ. However, optimizing TNF-α levels is essential, as excessive concentrations (>10 ng/mL) may induce cellular stress or apoptosis. Additionally, prolonged preconditioning may reduce anti-inflammatory cytokine production due to cellular homeostasis mechanisms. Literature suggests that TNF-α levels should not exceed 10 ng/mL [42,43] to prevent cytotoxicity, particularly when combined with IFN-γ.

This study found no significant variation in BDNF, GDNF, NGF, and VEGF secretion across the four secretome types, indicating that preconditioning did not affect growth factor production. While an increase was not expected, maintaining stable levels suggests successful preservation of factors essential for cellular health, growth, and proliferation, particularly in progenitor stem cells. The findings indicate that preconditioning did not significantly alter neuronal cell viability across different secretome types, aligning with the similar composition of sNEP, cytokines, and growth factors. This supports the previous study [44], who suggested that variations in secretome composition influence biological effects, whereas comparable compositions yield similar outcomes.

Notably, preconditioning with IFN-γ at a 10% dose resulted in the highest neuronal viability at 48 and 72 hours, approaching normal conditions. This suggests that IFN-γ preconditioning enhances the neuroprotective potential of hUC-MSC-derived secretome, making it a promising approach for improving neuronal survival. Cell viability depended on Aβ42 plaques, pro-inflammatory cytokines, anti-inflammatory cytokines, and growth factors. A limited increase in one or two factors, while others remained unchanged, did not ensure a cumulative or synergistic effect on neuronal survival. This study demonstrated a healthier microenvironment with increased anti-inflammatory cytokines, which reduced inflammation and likely optimized growth factor function. The synergy between these factors enhanced neuron-like cell viability, supporting neuronal survival, proliferation, and differentiation, thereby promoting tissue repair and regeneration.

TNF-α and IFN-γ should be administered sequentially due to their distinct roles. IFN-γ should be applied first to enhance CD10 expression on hUC-MSC, as it modulates immune responses and surface marker expression. Following IFN-γ preconditioning, the cells should be washed with phosphate-buffered saline (PBS) to remove residual IFN-γ, ensuring its effects do not interfere with subsequent TNF-α exposure. Fresh culture medium should then be added before introducing TNF-α as a new preconditioning agent. This step minimizes potential cross-interactions that could exacerbate inflammation.

Simultaneous administration may induce cytotoxicity and compromise MSC function through necroptosis and inflammatory signaling pathways. IFN-γ predominantly activates immune-related gene transcription, whereas TNF-α, if not carefully regulated, can trigger cell death [45,46]. To prevent excessive inflammation and preserve MSC immunomodulatory properties, TNF-α preconditioning should be restricted to a maximum of three hours [42,47].

IFN-γ preconditioning is the most effective strategy for sustaining long-term neuronal viability, particularly at 10% and 20% secretome doses. The combination of TNF-α and IFN-γ provides a synergistic effect but does not surpass IFN-γ alone at later time points. Un-preconditioned and TNF-α preconditioned secretome offer some benefits, but their effects are either transient or less potent, underscoring the superior role of IFN-γ in optimizing secretome therapeutic potential.

While these findings have limitations, their theoretical foundation is well established. To improve therapeutic efficacy, further optimization of IFN-γ and TNF-α preconditioning levels is essential, with careful management of potential toxicity risks. Future studies should refine IFN-γ and TNF-α administration, incorporate washing steps between preconditioning phases to prevent antagonistic effects, and determine the optimal duration for IFN-γ and TNF-α exposure. These optimizations are expected to significantly enhance sNEP production and increase levels of anti-inflammatory cytokines (IL-4, IL-10, and TGF-β) and growth factors (BDNF, GDNF, NGF, and VEGF) compared to non-preconditioned secretome.

Optimizing culture conditions, including temperature, pH, and oxygen levels (hypoxia), is crucial for enhancing cellular responses to IFN-γ and TNF-α, thereby improving sNEP, anti-inflammatory cytokine, and growth factor production. In vivo studies using AD animal models are essential to evaluate the safety, efficacy, and therapeutic mechanisms of hUC-MSC-derived secretome before clinical application.

Conclusion

Across all three doses (5%, 10%, and 20%), IFN-γ proved to be the most effective factor for hUC-MSC preconditioning, significantly enhancing neuronal cell viability, with its impact being particularly strong and sustained at higher doses (10% and 20%), where it consistently yielded the highest viability up to 72 hours post-therapy. Preconditioning with a combination of TNF-α and IFN-γ produced synergistic effects, particularly at 5% and 10%, but at 20%, IFN-γ alone was more effective, indicating a dose-dependent shift in effectiveness. TNF-α preconditioning alone showed stable and consistent effects across all doses but was less potent than IFN-γ alone or the TNF-α + IFN-γ combination in promoting long-term viability. Secretome derived from hUC-MSCs without preconditioning provided short-term benefits, particularly within the first 48 hours, but failed to sustain optimal neuronal viability over time. Therefore, for applications requiring long-term neuronal support, preconditioning with IFN-γ alone or in combination with TNF-α is the most effective strategy.

Ethics approval

This study has obtained ethical clearance in accordance with Ethical Clearance Certificate No. Ket-350/UN2.F1/ETIK/PPM.00.02/2024, dated March 4, 2024, issued by the Health Research Ethics Committee of Dr. Cipto Mangunkusumo National General Hospital - Faculty of Medicine, Universitas Indonesia.

Acknowledgments

We sincerely express our gratitude to the Stem Cell and Tissue Engineering Laboratory team at the Indonesia Medical Education and Research Institute (IMERI), Faculty of Medicine, Universitas Indonesia, for their invaluable support and technical assistance throughout this research. We also extend our deepest appreciation to the UKK PPM Integrated Laboratory team, Faculty of Medicine, Universitas Indonesia, for their guidance and access to research facilities that contributed significantly to the completion of this study.

Competing interests

All the authors declare that there are no conflicts of interest.

Funding

This research was funded by Mandaya Hospital Group, a hospital business group headquartered at Metland Boulevard Lot C-03, Metland Cyber City, Tangerang City, Indonesia.

Underlying data

Derived data supporting the findings of this study are available from the corresponding author upon request.

Declaration of artificial intelligence use

This study used artificial intelligence (AI) tools in the manuscript writing support using AI-based language model as Quillbot for paraphrasing, language refinement, and technical writing assistance. We confirm that all AI-assisted processes were critically reviewed by the authors to ensure the integrity and reliability of the results. The final decisions and interpretations presented in this article were solely made by the authors.

How to cite

Widaja E, Pawitan JA, Ramli Y. Therapeutic potential of hUC-MSC secretome preconditioned with IFN-γ and/or TNF-α: An in vitro study on Alzheimer's neuronal cell models. Narra J 2025; 5 (2): e2281 - http://doi.org/10.52225/narra.v5i2.2281.

References

1. Holtzman DM, Morris JC, Goate AM. Alzheimer's disease: The challenge of the second century. Sci Transl Med 2011;3(77):77sr1.
2. World Health Organization. Dementia. Available from: https://www.who.int/news-room/fact-sheets/detail/dementia. Accessed: 10 December 2024.
3. Alipour M, Nabavi SM, Arab L, *et al.* Stem cell therapy in Alzheimer's disease: Possible benefits and limiting drawbacks. Mol Biol Rep 2019;46(1):1425-1446.
4. Nelson PT, Braak H, Markesbery WR. Neuropathology and cognitive impairment in Alzheimer disease: A complex but coherent relationship. J Neuropathol Exp Neurol 2009;68(1):1-14.
5. Zhang Y, Chen H, Li R, *et al.* Amyloid β-based therapy for Alzheimer's disease: Challenges, successes and future. Signal Transduct Target Ther 2023;8(1):248.
6. Dang M, Chen Q, Zhao X, *et al.* Tau as a biomarker of cognitive impairment and neuropsychiatric symptom in Alzheimer's disease. Hum Brain Mapp 2023;44(2):327-340.
7. Li XL, Hu N, Tan MS, *et al.* Behavioral and psychological symptoms in Alzheimer's disease. BioMed Res Int 2014;2014:927804.
8. Reisberg B. 7 stages of Alzheimer's. Available from: https://www.alzinfo.org/understand-alzheimers/clinical-stages-of-alzheimers/. Accessed: 11 December 2024.
9. Lamptey RNL, Chaulagain B, Trivedi R, *et al.* A review of the common neurodegenerative disorders: Current therapeutic approaches and the potential role of nanotherapeutics. Int J Mol Sci 2022;23(3):1851.
10. Miao J, Ma H, Yang Y, *et al.* Microglia in Alzheimer's disease: Pathogenesis, mechanisms, and therapeutic potentials. Front Aging Neurosci 2023;15:1201982.
11. Leng F, Edison P. Neuroinflammation and microglial activation in Alzheimer disease: Where do we go from here?. Nat Rev Neurol 2021;17(3):157-172.
12. Maynard CJ, Bush AI, Masters CL, *et al.* Metals and amyloid-β in Alzheimer's disease. Int J Exp Pathol 2005;86(3):147-159.
13. Kim N, Lee HJ. Redox-active metal ions and amyloid-degrading enzymes in Alzheimer's disease. Int J Mol Sci 2021;22(14):7697.
14. Smith DG, Cappai R, Barnham KJ. The redox chemistry of the Alzheimer's disease amyloid beta peptide. Biochim Biophys Acta 2007;1768(8):1976-1990.
15. Wang DS, Dickson DW, Malter JS. *β*-amyloid degradation and Alzheimer's disease. BioMed Res Int 2006;2006(1):058406.

16. Rofo F, Ugur Yilmaz C, Metzendorf N, *et al.* Enhanced neprilysin-mediated degradation of hippocampal Aβ42 with a somatostatin peptide that enters the brain. Theranostics 2021;11(2):789-804.
17. Grimm MOW, Mett J, Stahlmann CP, *et al.* Neprilysin and Aβ clearance: Impact of the APP intracellular domain in NEP regulation and implications in Alzheimer's disease. Front Aging Neurosci 2013;5:98.
18. Lenz M, Krychtiuk KA, Brekalo M, *et al.* Soluble neprilysin and survival in critically ill patients. ESC Heart Fail 2022;9(2):1160-1166.
19. Jeong H, Kim OJ, Oh SH, *et al.* Extracellular vesicles released from neprilysin gene-modified human umbilical cord-derived mesenchymal stem cell enhance therapeutic effects in an Alzheimer's disease animal model. Stem Cells Int 2021;2021:5548630.
20. Wang S, Xiao Y, An X, *et al.* A comprehensive review of the literature on CD10: Its function, clinical application, and prospects. Front Pharmacol 2024;15:1336310.
21. Wang S, Jiang W, Lv S, *et al.* Human umbilical cord mesenchymal stem cells-derived exosomes exert anti-inflammatory effects on osteoarthritis chondrocytes. Aging 2023;15(18):9544-9560.
22. Xie Q, Liu R, Jiang J, *et al.* What is the impact of human umbilical cord mesenchymal stem cell transplantation on clinical treatment?. Stem Cell Res Ther 2020;11(1):519.
23. Goodarzi P, Alavi-Moghadam S, Payab M, *et al.* Metabolomics analysis of mesenchymal stem cells. Int J Mol Cell Med 2019;8 Suppl 1:30-40.
24. Xu J, Feng Z, Wang X, *et al.* hUC-MSCs exert a neuroprotective effect via anti-apoptotic mechanisms in a neonatal HIE rat model. Cell Transplant 2019;28(12):1552-1559.
25. Kang J, Guo Y. Human umbilical cord mesenchymal stem cells derived exosomes promote neurological function recovery in a rat spinal cord injury model. Neurochem Res 2022;47(6):1532-1540.
26. Pawitan J, Liem I, Budiyanti E. Umbilical cord derived stem cell culture: Multiple-harvest explant method. Int J PharmTech Res 2014;6(4):1202-1208.
27. Glpbio. FITC, Fluorescein isothiocyanate. Available from: https://www.glpbio.com/fitc-fluorescein-isothiocyanate.html. Accessed: 13 December 2024.
28. International Clinical Cytometry Society. What is MFI and how is it calculated?. Available from: https://www.cytometry.org/web/q_view.php?filter=Analysis+Techniques&id=152. Accessed: 13 December 2024.
29. Gorgun C, Ceresa D, Lesage R, *et al.* Dissecting the effects of preconditioning with inflammatory cytokines and hypoxia on the angiogenic potential of mesenchymal stromal cell (MSC)-derived soluble proteins and extracellular vesicles (EVs). Biomaterials 2021;269:120633.
30. Rogulska O, Vackova I, Prazak S, *et al.* Storage conditions affect the composition of the lyophilized secretome of multipotent mesenchymal stromal cells. Sci Rep 2024;14(1):10243.
31. Jammes M, Contentin R, Audigié F, *et al.* Effect of pro-inflammatory cytokine priming and storage temperature of the mesenchymal stromal cell (MSC) secretome on equine articular chondrocytes. Front Bioeng Biotechnol 2023;11:1204737.
32. Federer WT, King F. Variations on split plot and split block experiment designs. 1st ed. New Jersey: Wiley; 2007.
33. Todtenhaupt P, Franken LA, Groene SG, *et al.* A robust and standardized method to isolate and expand mesenchymal stromal cells from human umbilical cord. Cytotherapy 2023;25(10):1057-1068.
34. Dominici M, Le Blanc K, Mueller I, *et al.* Minimal criteria for defining multipotent mesenchymal stromal cells. The International Society for Cellular Therapy position statement. Cytotherapy 2006;8(4):315-317.
35. Liu Y, Studzinski C, Beckett T, *et al.* Circulating neprilysin clears brain amyloid. Mol Cell Neurosci 2010;45(2):101-107.
36. Sternlicht MD, Werb Z. How matrix metalloproteinases regulate cell behavior. Annu Rev Cell Dev Biol 2001;17(1):463-516.
37. Tsai CL, Chen WC, Hsieh HL, *et al.* TNF-α induces matrix metalloproteinase-9-dependent soluble intercellular adhesion molecule-1 release via TRAF2-mediated MAPKs and NF-κB activation in osteoblast-like MC3T3-E1 cells. J Biomed Sci 2014;21(1):12.
38. De Almeida LGN, Thode H, Eslambolchi Y, *et al.* Matrix metalloproteinases: From molecular mechanisms to physiology, pathophysiology, and pharmacology. Pharmacol Rev 2022;74(3):714-770.
39. Gonzalez-Avila G, Sommer B, Flores-Soto E, *et al.* Hypoxic effects on matrix metalloproteinases' expression in the tumor microenvironment and therapeutic perspectives. Int J Mol Sci 2023;24(23):16887.
40. Kapoor M, Chinnathambi S. TGF-β1 signalling in Alzheimer's pathology and cytoskeletal reorganization: A specialized Tau perspective. J Neuroinflammation 2023;20(1):72.

41. Von Bernhardi R, Cornejo F, Parada GE, Eugenín J. Role of TGFβ signaling in the pathogenesis of Alzheimer's disease. Front Cell Neurosci 2015;9:426.
42. Li X, Du W, Ma FX, *et al.* High concentrations of TNF-α induce cell death during interactions between human umbilical cord mesenchymal stem cells and peripheral blood mononuclear cells. PloS One 2015;10(5):e0128647.
43. Woznicki JA, Saini N, Flood P, *et al.* TNF-α synergises with IFN-γ to induce caspase-8-JAK1/2-STAT1-dependent death of intestinal epithelial cells. Cell Death Dis 2021;12(10):864.
44. Ribeiro CA, Fraga JS, Grãos M, *et al.* The secretome of stem cells isolated from the adipose tissue and Wharton jelly acts differently on central nervous system derived cell populations. Stem Cell Res Ther 2012;3(3):18.
45. Ren X, Ge M, Huo J, *et al.* IFN-γ and TNF-α synergistically induce mesenchymal stem/stromal cell death via RIPK1-independent necroptosis. Blood 2023;142 Suppl 1:5624-5624.
46. Shen J, Xiao Z, Zhao Q, *et al.* Anti-cancer therapy with TNFα and IFNγ: A comprehensive review. Cell Prolif 2018;51(4):e12441.
47. Sekenova A, Li Y, Issabekova A, *et al.* TNF-α preconditioning improves the therapeutic efficacy of mesenchymal stem cells in an experimental model of atherosclerosis. Cells 2023;12(18):2262.